

Magnetoelastic effect through coupled surface acoustic waves and spin waves in ferromagnetic Cobalt thin films

Author: Fiona Sosa Barth

*Facultat de Física, Universitat de Barcelona, Diagonal 645, 08028 Barcelona, Spain.**

Advisor: Ferran Macià Bros

Abstract: Magnetostriction is the property of a material to modify its shape upon a change of its magnetization. Conversely, the magnetoelastic effect accounts for the changes in magnetization after a material's deformation. Surface acoustic waves (SAW) are sound waves that travel parallel to the surface of an elastic material, thus creating a dynamic strain. It is known that SAW induced in a piezoelectric substrate can couple to a ferromagnetic material creating spin waves (SW), but has not yet been widely characterized in many materials. In this paper we want to observe the dynamic magnetoelastic effect in a Cobalt (Co) thin film deposited on a piezoelectric substrate capable to produce SAW. Transmission of SAW will be studied as a function of the magnetic field and the relative angle between field and SAW propagation. We observe absorption of SAW depending on the magnetic state of the Co thin film. This paper will furthermore be complemented with direct observation of SAW and SW through X-ray magnetic circular dichroism imaging. Thus the effects observed in the transmission of SAW can directly be correlated to SW and magnetic switching in the material.

I. INTRODUCTION

When a magnetic field is applied in a magnetic material a change of magnetization is induced, meaning a shift of the random direction domains. Some materials can present spontaneous deformation as a consequence of the tendency to rearrange their structure in order to reduce the total energy of the material [1]. This is called magnetostriction. The reverse effect, the magnetoelastic effect (ME), can change the magnetization through induced strain. This means magnetization can be controlled via strain with a much more efficient energy usage in comparison with the electric current inducing method necessary to create magnetic fields.

Dynamic strain can be applied in a material through surface acoustic waves (SAW). SAW are periodic perturbations on the surface of an elastic material, like a piezoelectric, in the GHz range. SAWs can interact with an adjacent material and couple to its magnetization [2], creating spatial variations at the nano- and microscale.

The possibility of coupling SAW with magnetization has also been studied in recent years in piezoelectric-ferromagnetic heterostructures [3–10]. The use of high frequency range and small dimensions combined with low-power signal processing needs has awakened huge interest because of its great adaptability to modern technologies. For example, SAW can be used for radio frequency (RF) filters and other signal processing acoustoelectric devices [7, 11], as well as the control of interfacing elementary excitations in solid-state quantum systems like coupling to defect centers [12, 13] and semiconductor structures of small dimensions [14–16]. The characterized

materials have been mainly composites with strong ME properties and combination layering of those [8, 17, 18]. Cobalt, known for its also strong magnetic response, but with a much lower ME coupling than the mentioned materials above, has yet not been thoroughly studied for SAW-magnetization coupling.

In this paper we characterize the response of Cobalt (Co). The transmission of SAW is measured at room temperature as a function of the strength of the external magnetic field \mathbf{H}_0 and the relative angle θ between SAW and \mathbf{H}_0 . In addition, this paper shows X-rays photoelectron microscopy imaging of the heterostructure. Magnetic oscillations caused by SAW will be observed through X-ray magnetic circular dichroism imaging together with the propagating SAW.

II. THEORY

Here we briefly introduce the main mathematical equations for the magnetization dynamics induced by the magnetoelastic effect (ME). Surface acoustic waves (SAW) create periodic strain upon the elastic material's structure and propagate with a characteristic velocity for sound waves around $v_s = 4000 \frac{m}{s}$ [19]. When propagating, SAW induce periodic magnetization changes to the neighbouring ferromagnetic material. This oscillations are called spin waves (SW) and can be quantified into magnons, quasiparticles. The magnetization dynamics induced by ME can be described by the Landau-Lifshitz-Gilbert equation (LLG)

$$\frac{d\mathbf{M}}{dt} = -\gamma\mu_0(\mathbf{M} \times \mathbf{H}_{\text{eff}}) + \frac{\alpha}{M_S}(\mathbf{M} \times \frac{d\mathbf{M}}{dt}) \quad (1)$$

with γ the gyromagnetic ratio, μ_0 the vacuum permeability, \mathbf{H}_{eff} the effective magnetic field, \mathbf{M} the mag-

*Electronic address: fsosabar7@alumnes.ub.edu

netization, M_S the saturation magnetization and α the Gilbert damping constant. The effective magnetic field has contributions from the external bias field \mathbf{H}_0 , the magnetostatic field \mathbf{H}_{mag} , the exchange field \mathbf{H}_{ex} and the magnetoelastic field \mathbf{H}_{me} [2].

The solution of Eq. 1 for \mathbf{M} describes effective precessing with a progressive lower amplitude around \mathbf{H}_{eff} direction axis due to energy loss and described through damping processes [20] (See Fig. 1). If \mathbf{M} and \mathbf{H}_{eff} are in parallel directions, meaning $\theta = 0^\circ$, \mathbf{H}_{eff} does not exert torque upon the magnetization \mathbf{M} which will consequently not precess. The torque is maximum for perpendicular direction, $\theta = 90^\circ$. For large enough fields the magnetization is saturated and has enough energy not to be perturbed by the lattice motion of SAW.

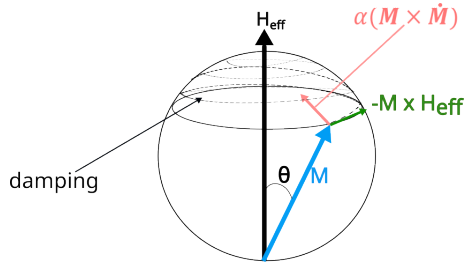


FIG. 1: Magnetization dynamics for a magnetic moment (blue) in a magnetic effective field (black) in the Landau-Lifshitz-Gilbert equation. The forces acting over the magnetization produce precessing around the magnetic field, in green, and aligning to the effective field direction (damping), in orange.

SAW, needed for ME effect, can be created in elastic materials such as piezoelectrics, through an interdigital transducer (IDT). Here a bidirectional IDT has been used, which consists of a periodical alignment of multiple electrode strips connected to a bus-bar which is interspersed in a comb-like shape to a second same-built structure (See Fig. 2). When a radio-frequency (RF) voltage is applied between the two IDT bus-bars a periodic strain is generated by the electric field (piezoelectric effect). The strain waves will not cancel each other out only when the IDT period corresponds to an integer multiple of the SAW wavelength [21]. The frequency of the SAW created follows the relation $f = \frac{n \cdot v}{d} = \frac{v_s}{\lambda_{\text{SAW}}}$, with n an integer, v and λ_{SAW} the velocity and wavelength of SAW respectively and d the distance between the electrode strips. A second IDT will be found at the other end of the material to convert, through inverse piezoelectric effect, the propagating SAW again into a voltage signal.

SAW can couple to magnetization because lattice motion deflects the atoms from their equilibrium position, inducing a change in their electronic states which are responsible for the magnetization. Thus, an additional magnetic field induced by SAW is accounted in Eq. 1. This field is the anisotropic magnetoelastic field \mathbf{H}_{me} ,

which points to the SAW propagation direction and depends on the magnetization [4]. It can be approximately described with the elastodynamic equations:

$$E_{\text{me}} \propto -aM_x^2 \quad (2)$$

$$\mathbf{H}_{\text{me}} = \frac{\partial E_{\text{me}}}{\partial \mathbf{M}} \propto -2aM_x \hat{\mathbf{x}} \quad (3)$$

It is worth noting that the anisotropic magnetoelastic energy does not change under an inversion of the magnetization ($E_{\text{me}}(\mathbf{M}) = E_{\text{me}}(-\mathbf{M})$). Combining Eq. 3 with Eq. 1, we can understand when SW appear. For parallel directions of \mathbf{M} and \mathbf{H}_{eff} the left term of Eq. 3 will be canceled. In the case of perpendicular direction \mathbf{H}_{me} will also be zero (considering only M_x dependence). In both cases no torque is applied upon \mathbf{M} and no SW will be seen. Hence, SW are predicted for $0^\circ < \theta < 90^\circ$.

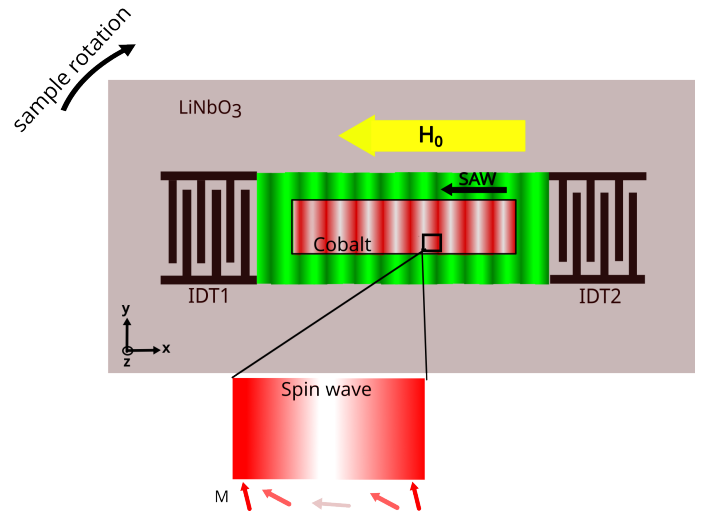


FIG. 2: Heterostructure of piezoelectric substrate of LiNbO₃ in grey, two IDTs in black that can create surface acoustic waves (SAW). In green the created SAW travelling in between the two IDTs. In red the spin waves created upon the cobalt thin film, which is delimited by a black line, and the external magnetic field in yellow.

The magnetization dynamics are of great importance to understand when changes in the SAW signal will be observed. In the first place, SAW attenuation can be observed when ME coupling transfers energy from the elastic to the magnetic system. The magnetic system absorbs energy when the magnetization precession frequency matches the SAW frequency, meaning resonance [4, 5]. SAW absorption will also have a dependence on the strength of \mathbf{H}_0 , which conditions the precession amplitude and thus the frequency.

As for the second part of this paper, direct imaging through photoemission electron microscopy (PEEM) of magnetic domains will be shown. The images present spatially and temporally resolved electrical contrast using X-ray magnetic circular dichroism (XMCD) [3, 22, 23].

XMCD uses circularly polarized X-rays to characterize ferro- and ferrimagnetic materials: X-rays get absorbed in different magnitude depending on the relative orientation of their helicity to the direction of the magnetization of the ferromagnet \mathbf{M} . XMCD contrast thus is obtained by keeping the magnetization direction constant and changing the helicity of the circular polarization. Simultaneous imaging of strain and magnetization is possible by synchronizing SAW frequency to the X-rays pulse repetition rate [24, 25]. The resulting image shows magnetic domains from the first nanometers of the sample's surface [9] with a resolution up to 40 nm.

III. RESULTS

The analyzed sample is a heterostructured device of a 10 nm thin cobalt (Co) film deposited on a LiNbO_3 piezoelectric substrate. The Co was grown in a polycrystalline structure in several strips over the sample. The strips measure $4 \text{ mm} \times 100 \mu\text{m}$. On top of the sample and at its edges the IDTs connect to the electric signal and create SAW which propagate parallel to the piezoelectric's surface. The IDT are numbered as IDT1 and IDT2, which work at different frequencies. In this experiment, the SAW signal was emitted and received through IDT2, with a frequency of 1 GHz. The set up is shown in Fig. 2. The incoming and outgoing signal is controlled with a programmable network analyzer (PNA), which will give the transmission of SAW for each external magnetic field \mathbf{H}_0 .

To characterize SW in the sample we start by analysing the dependence of the transmission (and through it the absorption) of SAW to \mathbf{H}_0 . Additionally, we change the respective angle of \mathbf{H}_0 to the SAW propagation direction by moving the sample for a fixed direction of \mathbf{H}_0 (See Fig. 2). The angle between SAW and \mathbf{H}_0 is considered approximately the same as the angle θ between \mathbf{M} and \mathbf{H}_{eff} due to much bigger external magnetic fields than ME fields. In Fig. 3 we can observe the relative SAW signal loss S_{12} for the returning signal in response to \mathbf{H}_0 . The maximum loss of SAW amplitude is found at symmetrical resonant magnetic fields, which can be seen in Fig. 3 for $\theta = 13^\circ$. For angles outside the strong SW absorption range ($-57^\circ, -27^\circ$) a narrow peak is clearly seen due to magnetic switching. The obtained data is shown more extensively in Fig. 4, where transmission is seen from -30° to 30° with a fourfold symmetry for the minimum transmission at approximately $\theta = 10^\circ$ and $\mathbf{H}_0 = \pm 3 \text{ mT}$. Minimum transmission of the magnetic fields appears for opposite direction fields since the anisotropic magnetoelastic field does not change under an inversion of the magnetization ($E_{\text{me}}(\mathbf{M}) = E_{\text{me}}(-\mathbf{M})$). At zero angle, a reduction of the absorption magnitude can be seen but it does not tend to zero due to other terms not mentioned in Eq. 3.

Furthermore, the strength of the induced SW can

be obtained through the transmission minima of SAW shown in Fig. 4. We reach about 0.07 dB for the maximum change between incoming and outgoing SAW transmission signal. Compared to a nickel heterostructured device, it is about an order of magnitude smaller [2, 10, 26]. The order of magnitude of the absorption is reasonable when considered that Co has weaker magnetoelastic properties than Ni [27]. Additionally, a non-reciprocal behaviour can be seen between the positive and negative field transmission: the depth of the peak is not equal for both fields. Even so, the shown results follow the dynamic magnetization behaviour mentioned in the introduction. Maximum dynamic magnetization effect is thus observed at $0^\circ < \theta < 90^\circ$.

In Fig. 4 the magnetic field was swept from negative to positive fields. In this figure a strong absorption can be seen on the right side of the fourfold symmetry at approximately 2 mT. This additional absorption, almost angle independent, is due to magnetic switching. Magnetic domains will appear due the external magnetic field. SW propagating through the magnetic sample can interact with magnetic domain walls and hence have energy loss [28, 29]. We will be able to relate this effect to the XMCD images shown below. For a ferromagnet, switching will not be at zero magnetic field, which is also observed.

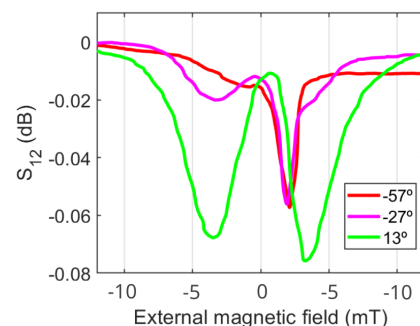


FIG. 3: The difference of the sending and receiving SAW signal, S_{12} (dB), as a function of the external magnetic field (mT), for several angles between SAW and the external magnetic field. For -57° and -27° switching is observed as a narrow peak.

In the second part of this paper we show direct imaging of SAW and SW. The following images have been obtained through a photoemission electron microscopy (PEEM) using the synchrotron ALBA X-ray source beamline CIRCE 24. Firstly, XMCD is shown for Co (corner) and LiNbO_3 in Fig. 5. Static magnetic field is applied increasing the magnitude through Fig. 5 a) to d). The induced change in magnetization by the external field in the ferromagnetic Co sample can be seen by the reduction of the dark magnetization domain (anti parallel to the magnetic field) until saturation is reached (Fig. 5 d)). In this figure, over the piezoelectric substrate, SAW can be seen only with a small contrast as they have been

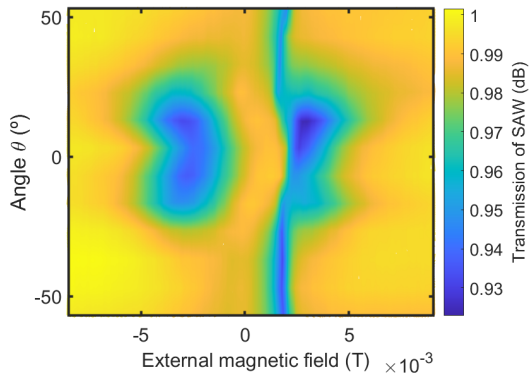


FIG. 4: Transmission of SAW (dB) in dependence with the external magnetic field (T), for several angles θ ($^\circ$) between the sample and the external magnetic field. Minimum transmission of SAW in dark blue. The vertical line shows magnetic switching.

almost cancelled out through the XMCD image processing. We can see a correlation between magnetic shifting absorption, shown simultaneously in Fig. 3 and Fig. 4, and the magnetic fields for the magnetic domain shifting in Fig. 5. Both are seen at approximately 2 mT.

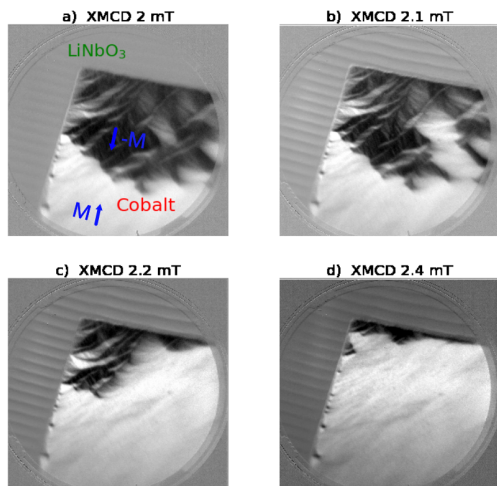


FIG. 5: XMCD images with a PEEM detector of a LiNbO_3 substrate and a Co thin film. The white and black contrast are opposite magnetic domains. From images a) to d) we have increasing magnetic field and magnetic shifting is shown.

Furthermore, when combining two XMCD images with a shifting of 180° SAW phases, high contrast images for SW are obtained. This is shown in Fig. 6. Both SAW and SW can be seen at the piezoelectric substrate and at the Co film respectively. SW display less contrast as SAW, reasonable as SW are related to SAW through a coupling constant depending on the material and can also quickly lose energy (small propagation length). The maxima and minima of SAW and SW are spatially correlated although some small shifting can be seen due to

the piezoelectric to ferromagnetic transition.

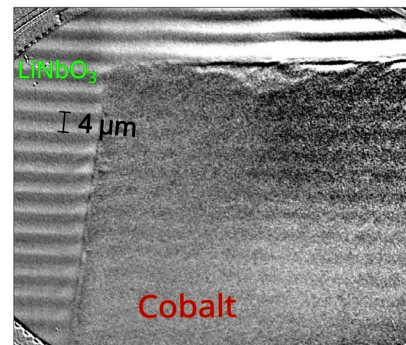


FIG. 6: Surface acoustic waves (material outside of corner) on LiNbO_3 substrate and spin waves (material inside corner) over Co film for the magnetic field created by a current of -2.6 mT. The distance between two maxima is $4 \mu\text{m}$.

IV. CONCLUSIONS

A basic characterization of SAW and the changes of magnetization that they induce, SW, have been provided in this work for a thin Co film deposited on a LiNbO_3 piezoelectric substrate. The response of SW to an external magnetic field has been observed, through SAW absorption, for symmetric fields ($\pm \mathbf{H}_0$). The magnitude of the absorption is not symmetrical for both peaks, thus indicating nonreciprocal interaction between \mathbf{M} and SAW propagation [7]. Furthermore, the behaviour of SW resonance in dependence with the relative angle from SAW to \mathbf{H}_0 , θ , is also shown. Absorption is seen from -30° to 30° with maximum absorption for a fourfold symmetry at approximately $\theta = 10^\circ$, which is in accordance with the predicted model. Additionally, magnetic switching can be observed through SAW absorption and through direct XMCD imaging at approximately the same magnetic field, 2 mT. Finally, we are able to show spatially and time correlated images of SAW and SW propagation at the piezoelectric and thin cobalt's film surface respectively.

To reach deep understanding of the ME effect in thin cobalt films we would have to analyze the obtained data not only qualitatively but using the complete magnetization and strain equations. It would allow us to characterize quantitatively thin Co films for ME effects, which are not yet entirely studied. Hence, it would be interesting to continue this research, also at higher SAW frequencies, as they can be of great interest for faster and more efficient technology.

Acknowledgments

I would like to thank my tutor Ferran Macià for the help provided and for always being able to dispose of his time. The enthusiasm about the subject has reached me and made me pursue my best for this thesis. Also

special thanks to Marc Rovirola, M. Waqas and the UB magnetism group for the support in the laboratory, for being able to participate in their measurements in ALBA synchrotron and to use the resulting data. I finally want to thank my family and friends for their support.

-
- [1] E. W. Lee. 'Magnetostriction and Magnetomechanical Effects'; *Rep. Prog. Phys.* 18 184 (1955)
- [2] X. Li, D. Labanowski, S. Salahuddin, C. S. Lynch. 'Spin wave generation by surface acoustic waves'; *J. Appl. Phys.* 122, 043904 (2017)
- [3] B. Casals, N. Statuto, M. Foerster, A. Hernández-Mínguez, R. Cicheler, P. Manshausen, A. Mandziak, L. Aballe, J. M. Hernández, F. Macià. 'Generation and Imaging of Magnetoacoustic Waves over Millimeter Distances'; *Phys. Rev. Lett.* 124, 137202 (2020)
- [4] M. Weiler, L. Dreher, C. Heeg, H. Huebl, R. Gross, M. S. Brandt, and S. T. B. Goennenwein. 'Elastically driven ferromagnetic resonance in nickel thin films'; *Phys. Rev. Lett.* 106, 117601 (2011)
- [5] M. Weiler, H. Huebl, F. S. Goerg, F. D. Czeschka, R. Gross, and S. T. B. Goennenwein. 'Spin pumping with coherent elastic waves'; *Phys. Rev. Lett.* 108, 176601 (2012)
- [6] L. Thevenard, C. Gourdon, J. Y. Prieur, H. J. von Bardeleben, S. Vincent, L. Becerra, L. Largeau, and J.-Y. Duquesne. 'Surface-acoustic-wave-driven ferromagnetic resonance in (Ga,Mn)(As,P) epilayers'; *Phys. Rev. B* 90, 094401 (2014)
- [7] A. Hernández-Mínguez, F. Macià, J. M. Hernández, J. Herfort, and P. V. Santos. 'Large nonreciprocal propagation of surface acoustic waves in epitaxial ferromagnetic/semiconductor hybrid structures'; *Phys. Rev. Applied* 13, 044018 (2020)
- [8] X. Liang, C. Dong, H. Chen, et al. 'A Review of thin-film magnetoelastic materials for magnetoelectric applications'; *Sensors (Basel)*; 20(5):1532 (2020)
- [9] P. Fischer, H. Ohldag. 'X-rays and magnetism'; *Rep. Prog. Phys.* 78 094501 (2015)
- [10] D. Labanowski, A. Jung, S. Salahuddin. 'Power absorption in acoustically driven ferromagnetic resonance'; *Appl. Phys. Lett.* 108, 022905 (2016)
- [11] C. K. Campbell, 'Surface Acoustic Wave Devices for Mobile and Wireless Communications'; edited by R. Stern and M. Levy (Academic Press, Inc., San Diego) (1998)
- [12] S. Lazić, A. Espinha, S. Pinilla Yanguas. 'Dynamically tuned non-classical light emission from atomic defects in hexagonal boron nitride'; *Commun. Phys.* 2, 113 (2019)
- [13] X. Shen, L. Zhao, P. Huang, X. Kong, L. Ji. 'Atomic spin and phonon coupling mechanism of nitrogen-vacancy center'; *Acta Phys. Sin.*, 70(6): 068501 (2021)
- [14] R. McNeil, M. Kataoka, C. Ford. 'On-demand single-electron transfer between distant quantum dots'; *Nature* 477, 439–442 (2011)
- [15] D. A. Golter, T. Oo, M. Amezcua, K. A. Stewart, H. Wang. 'Optomechanical quantum control of a nitrogen vacancy center in diamond'; *Phys. Rev. Lett.* 116, 143602 (2016)
- [16] O. Couto, S. Lazić, F. Iikawa. 'Photon anti-bunching in acoustically pumped quantum dots'; *Nature Photon* 3, 645–648 (2009)
- [17] M. J. PourhosseiniAsl, Z. Chu, X. Gao, S. Dong. 'A hexagonal-framed magnetoelectric composite for magnetic vector measurement'; *J. Phys. D: Appl. Phys.* 51 243001 (2018)
- [18] G. Komoriya, G. Thomas. 'Magnetoelastic-surface waves on YIG substrate'; *J. Appl. Phys.* 50, 6459 (1979)
- [19] M. Foerster, N. Statuto, B. Casals, A. Hernández-Mínguez, S. Finizio, A. Mandziak, L. Aballe, J. M. Hernández, F. Macià. 'Quantification of propagating and standing surface acoustic waves by stroboscopic X-ray photoemission electron microscopy'; *J. Synchrotron Rad.* 26, 184–193 (2019)
- [20] M. Getzlaff. 'Fundamentals of Magnetism' (1st ed. 2008); Berlin, Heidelberg: Springer Berlin Heidelberg
- [21] Ky. Hashimoto. 'Interdigital Transducers', in *Surface Acoustic Wave Devices in Telecommunications*; Springer, Berlin, Heidelberg (2000)
- [22] L. Aballe, M. Foerster, E. Pellegrin, J. Nicolas, S. Ferrer. 'The ALBA spectroscopic LEEM-PEEM experimental station: layout and performance'; *J. Synchrotron Radiat.* 22, 745 (2015)
- [23] J. Stohr and H. Siegmann. 'Magnetism: from fundamentals to nanoscale dynamics' (Springer Berlin Heidelberg, 2006), Vol. 152.
- [24] M. Foerster, L. Aballe, J.M. Hernández, et al. 'Sub-nanosecond magnetization dynamics driven by strain waves'; *MRS Bulletin* 43, 854–859 (2018)
- [25] M. Foerster, J. Prat, V. Massana, N. Gonzalez, A. Fontserè, B. Molas, O. Matilla, E. Pellegrin, L. Aballe. 'Custom sample environments at the ALBA XPEEM'; *Ultramicroscopy* 171, 63 (2016)
- [26] D. Labanowski, A. Jung, S. Salahuddin. 'Effect of magnetoelastic film thickness on power absorption in acoustically driven ferromagnetic resonance'; *Appl. Phys. Lett.* 111, 102904 (2017)
- [27] C. Duan, J. P. Velev, R. F. Sabirianov, Z. Zhu, J. Chu, S. S. Jaswal, E. Y. Tsymlal. 'Surface magnetoelectric effect in ferromagnetic metal films'; *Phys. Rev. Lett.* 101, 137201 (2008)
- [28] D. Castilla, R. Yanes, M. Sinusía et al. 'Magnetization process of a ferromagnetic nanostrip under the influence of a surface acoustic wave'; *Sci. Rep.* 10, 9413 (2020)
- [29] M. Foerster, F. Macià, N. Statuto, et al. 'Direct imaging of delayed magneto-dynamic modes induced by surface acoustic waves'; *Nat. Commun.* 8, 407 (2017)
- [30] R. F. Wiegert, M. Levy. 'Temperature dependence and annealing effects on magnetoelastic SAW attenuation and magnetoresistance in Ni films'; *IEEE Trans. Magn.*, vol. 37, no. 4, pp. 2708–2711 (2001)